

Complex evolution processes in the upper feeding system of Mt. Etna (Italy) as revealed by the geochemistry of recent lavas

MARCO VICCARO, CARMELO FERLITO and RENATO CRISTOFOLINI*

Università degli Studi di Catania, Dipartimento di Scienze Geologiche, Corso Italia, 57, I-95129, Catania (Italy)

Submitted, June 2008 - Accepted, October 2008

ABSTRACT. — This comprehensive review, based on a database constituted of original major element compositions for mineral phases together with already published geochemical and isotopic data for lavas and tephra, discusses some aspects of the 2001 eruption at Mt. Etna aimed at clarifying pre- and sin-eruptive differentiation processes. Lavas and tephra with rather distinct petrographic and geochemical features were being emitted for about 20 days of intense activity from two different fracture systems along the southern slopes of the volcano, namely: i) a NNW-SSE oriented one, active at the South East crater (3100 m a.s.l.) and Piano del Lago (2950-2650 m a.s.l.) areas, hereafter called SE-PL; ii) a N-S oriented one, with vents at Mts. Calcarazza (2100 m a.s.l.) and Laghetto (2550 m a.s.l.) areas. Lavas from the SE-PL fractures are characterized by a Porphyritic Index (P.I.) ~30-40 with abundant oscillatory-zoned plagioclase, whereas those from the N-S fracture (both at the Calcarazza and Laghetto areas) are oligophytic (P.I. ~10-20) and characterized by i) the peculiar occurrence of Mg-hastingsite megacrysts and ii) large amounts of quartzarenite xenoliths. Core-rim profiles on plagioclase and clinopyroxene phenocrysts from the N-S fracture exhibit no significant compositional changes in the early-emitted products at the Calcarazza

area (2100 m a.s.l.), whereas An% and Mg# markedly increase at the phenocryst rims of plagioclase and clinopyroxene respectively in the late-emitted lavas by the Laghetto vent (2550 m a.s.l.). The latter products exhibit a more primitive character together with a distinct trace element signature if compared to the lavas emitted from the 2100 m vent. Sr, Nd, Pb and O isotopic compositions reveal also a marked change towards higher Sr isotope ratios and lower Nd-Pb-O ones in the late-emitted volcanics of the Laghetto vent. All these features, exclusive of this vent, support a model of an uprise of more primitive, volatile-rich and isotopically distinct magma into the deeper portion of a closed, 6 km deep, reservoir shortly before the eruption, which led to mixing of the new magma with the residing one. Moreover, major element compositions of residual glasses in tephra grains coming from the Laghetto vent, indicate that, before magma input and mixing, a volatile influx occurred in the system, which caused an enrichment in Ti, Fe, P, K and volatiles (Cl, H₂O, etc.) in the northern part of the closed magma body. Volcanological observations suggest that this complex interaction strongly controlled the eruptive behaviour at the Laghetto vent, where the mixed, volatile-enriched products were emitted.

RIASSUNTO. — Questa review, basata su dati originali di elementi maggiori per le fasi minerali e dati geochimici ed isotopici già pubblicati per

* Corresponding author, E-mail: rcristof@unict.it

lave e prodotti piroclastici, discute alcuni aspetti dell'eruzione del 2001 all'Etna al fine di chiarirne i processi di differenziazione pre- e sin-eruttivi. Lave e prodotti piroclastici con caratteri petrografici e geochimici relativamente distinti sono stati emessi durante circa 20 giorni di intensa attività da due sistemi di fratture indipendenti sul fianco meridionale del vulcano: i) un sistema orientato NNW-SSE, presso il Cratere di Sud-Est (3100 m s.l.m.) e nell'area di Piano del Lago (2950-2650 m s.l.m.), denominato SE-PL; ii) un altro sistema orientato N-S, presso le aree dei Monti Calcarazzi (2100 m s.l.m.) e Laghetto (2550 m s.l.m.). Le lave dalle fratture del sistema SE-PL sono caratterizzate da un Indice di Porfiricità (P.I.) ~30-40 con abbondanti plagioclasie con zonature oscillatorie, mentre i prodotti dal sistema N-S (sia nell'area dei Calcarazzi che al Laghetto) sono oligofirici (P.I. ~10-20) e caratterizzati da: i) la presenza singolare di megacristalli di Mg-hastingsite e ii) notevoli quantità di xenoliti quarzarenitici. I profili nucleo-bordo su fenocristalli di plagioclasio e clinopirosseno dalla frattura N-S non mostrano significative variazioni composizionali nei prodotti emessi durante le prime fasi nell'area dei Calcarazzi (2100 m s.l.m.), mentre marcati aumenti in An% e Mg# si osservano al bordo dei fenocristalli erutti durante le fasi tardive al cratere Laghetto (2550 m s.l.m.). Questi ultimi prodotti mostrano un carattere più primitivo associato a differenti contenuti di elementi in traccia in confronto alle lave emesse dal centro di 2100 m. Inoltre, i rapporti isotopici di Sr, sono più elevati e quelli di Nd, Pb e O più bassi nelle vulcaniti emesse durante le fasi finali dell'eruzione al Laghetto. L'insieme di questi dati, riferibili esclusivamente ai prodotti di questo apparato, supportano un modello in cui una ricarica di magma più primitivo, ricco in volatili e isotopicamente distinto è avvenuta poco prima dell'eruzione nelle porzioni inferiori di una camera magmatica chiusa, profonda ~6 km, con conseguente mescolamento tra il nuovo magma e quello stazionante. Inoltre, le composizioni degli elementi maggiori in vetri residuali dei prodotti piroclastici erutti al cratere Laghetto indicano che, prima della ricarica di magma e mescolamento, un flusso di volatili ha interessato il sistema residente, portando ad un arricchimento in Ti, Fe, P, K e volatili (Cl, H₂O ecc ...) nella porzione settentrionale della camera magmatica chiusa. Le osservazioni vulcanologiche suggeriscono che questo complesso processo di interazione ha fortemente controllato il comportamento eruttivo al centro del Laghetto, dove sono stati emessi i prodotti ibridizzati e arricchiti in volatili.

KEY WORDS: *Mount Etna, 2001 eruption, magma mixing, volatile exsolution, degassing*

INTRODUCTION

The Etna 2001 eruption, which occurred from July 13 to August 9, can be considered among the best documented and investigated episodes occurred in the last decades. It was characterized by two simultaneously eruptive fracture systems, developed on the upper southern flank of the volcano (Fig. 1; Behncke and Neri, 2003). Fractures of the upper NNW-SSE system developed between the South East crater and the Piano del Lago area between 3100 m and about 2650 m a.s.l. (SE-PL system). The lower N-S system started to erupt at an elevation of 2100 m in the Calcarazzi area and later at 2550 m in the Laghetto area. Activity at the latter site turned to be highly explosive, and may certainly be regarded as one among the most violent in the historical record of Mt. Etna (Romano, 1982; Branca and Del Carlo, 2004). Even if the overall volume of lavas and tephra is estimated in the order of only $\sim 30 \times 10^6$ m³ (Behncke and Neri, 2003; Clocchiatti *et al.*, 2004), the anomalous development of eruptive dynamics, along with some uncommon petrographic and geochemical features (e.g., the presence of amphibole; Viccaro *et al.*, 2007), have led many authors to produce a vast and multidisciplinary literature, which points out the intriguing character of such eruption (Clocchiatti *et al.*, 2004; Métrich *et al.*, 2004; Monaco *et al.*, 2005; Allard *et al.*, 2006; Viccaro *et al.*, 2006; Ferlito *et al.*, 2008a). However, a unique model is still matter of considerable debate some 8 years after the eruption. For this reason, using all the available geochemical data and providing new major element data for plagioclase and clinopyroxene, we present here a comprehensive model, in order to clarify as far as possible the entire set of pre- and sin-eruptive differentiation processes occurred within the shallow feeding system, also providing new perspectives for considering sources of hazard induced by inputs of primitive, volatile-rich magmas in basaltic volcanoes.

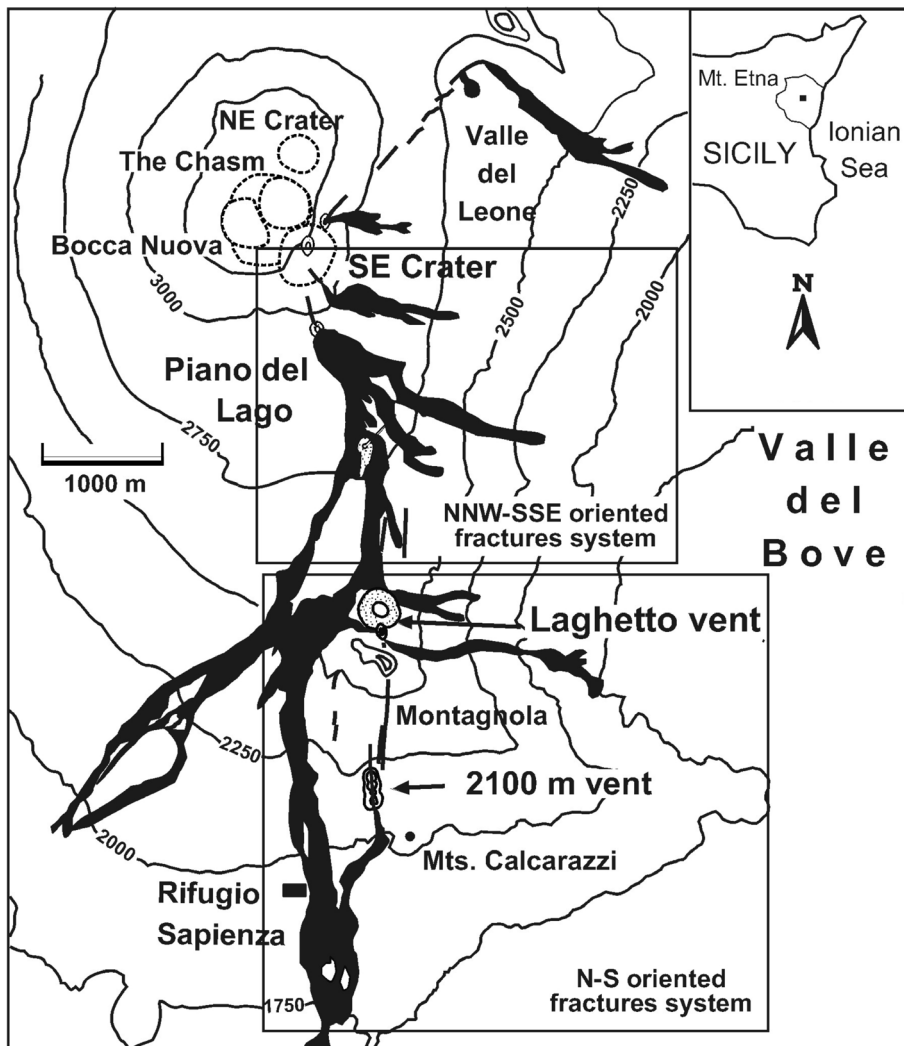


Fig. 1 – Sketch map of lava flows and scoria cones active during the 2001 eruption (modified after Viccaro *et al.*, 2006).

ANALYTICAL PROCEDURES

Lava flow units were sampled taking into account dates and sites of their emission. A total of 25 rock samples was subject to petrographic examination and in situ mineral microanalysis. Readers can refer to Viccaro and Cristofolini (2008) for details on procedures followed for whole rock analyses.

Original data for major element compositions of mineral phases were obtained by means of a

Cameca SX-50 electron microprobe equipped with four wavelength dispersive spectrometers (WDS) and one energy dispersive spectrometer (EDS) at the CNR-IGG, Section of Padova (Italy). Plagioclase and clinopyroxene phenocrysts were analyzed along core-rim transects with steps of about 15 μm . Operating conditions were set at 15 kV accelerating voltage, 15 nA beam current, peak counting times of 15 seconds and 2-3 μm focused electron beam. Used standards included: albite for

Na, Al_2O_3 for Al, periclase for Mg, wollastonite for Si and Ca, orthoclase for K, Fe_2O_3 for Fe, MnTiO_3 for Mn and Ti, Cr_2O_3 for Cr. The accuracy is $\sim 0.5\%$ for abundances > 15 wt%, $\sim 1\%$ for abundances around 5 wt% and $\sim 20\%$ for abundances around 0.5 wt%, and the precision is given as better than 1% for SiO_2 , Al_2O_3 , FeO, MgO and CaO and better than 3% for TiO_2 , Cr_2O_3 , MnO, Na_2O and K_2O .

PETROGRAPHY AND MINERAL CHEMISTRY

Lavas erupted by the NNW-SSE-oriented and the N-S-oriented fracture systems are markedly distinct in their textures and modal compositions.

SE-PL lavas are mesophyric with a seriate texture and Porphyritic Index (P.I.) ~ 30 -40. Their mineral assemblage consists of phenocrysts of plagioclase (~ 20 vol.%), clinopyroxene (~ 10 vol.%), Fo_{76-70} olivine (< 5 vol.%) and Ti-magnetite (< 5 vol.%). All phenocrysts occur in a hyalopilitic groundmass. Plagioclase phenocrysts in SE-PL lavas are oscillatory-zoned (An_{80-52}) and do not present sieve textures or marked spikes in their An% contents along the analyzed transects (Fig. 2; Table 1). Clinopyroxene compositions fall in the augite field (Morimoto, 1988) next to the boundary with diopside, and compare well with those of other pyroxenes of Etnean alkaline lavas (Cristofolini and Tranchina, 1980; Cristofolini *et al.*

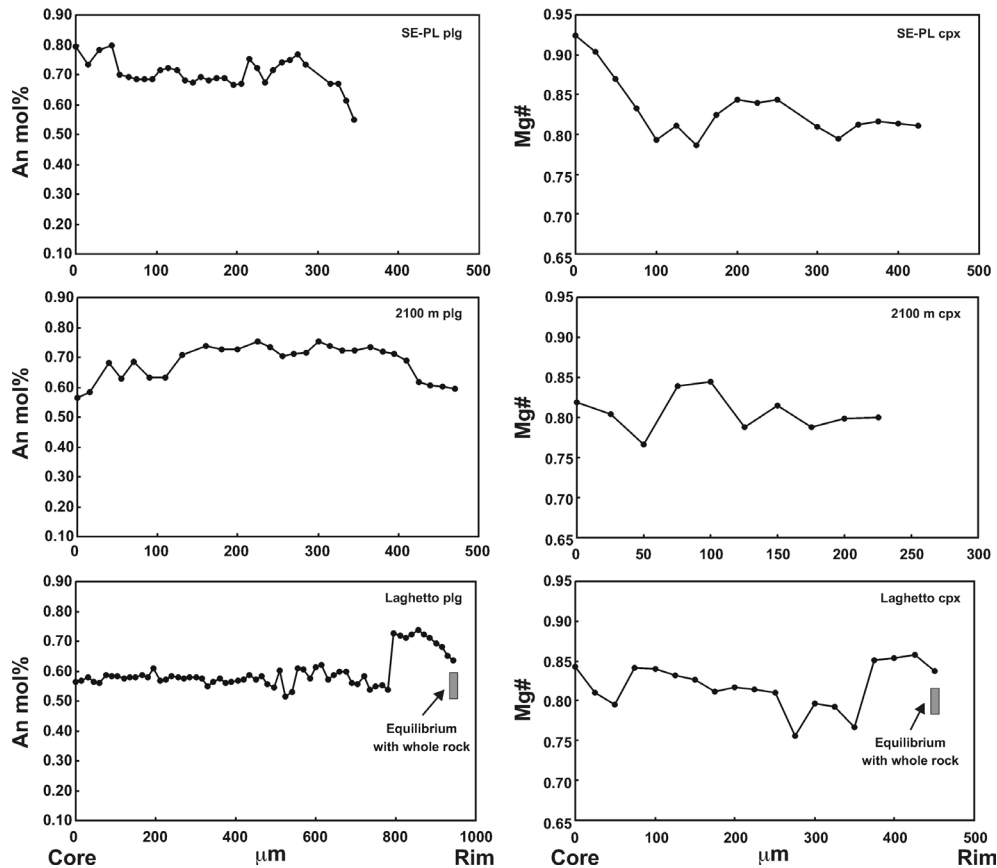


Fig. 2 – Core-rim compositional profiles for phenocrysts of plagioclase (left column) and clinopyroxene (right column) emitted at the SE-PL, 2100 m and Laghetto vents. Shaded rectangles indicate the An% and Mg# of plagioclase and clinopyroxene respectively expected in equilibrium with the Laghetto lava composition.

TABLE 1 — Plagioclase compositions of representative phenocrysts in lavas of the 2001 eruption

SE-PL	SiO ₂	TiO ₂	Al ₂ O ₃	FeO	MgO	Na ₂ O	K ₂ O	CaO	Total	An	Ab	Or	
vents	48.49	0.17	32.62	0.87	0.36	1.97	0.29	15.15	99.92	0 µm (core)	0.79	0.19	0.02
	50.11	0.20	31.43	0.99	0.33	2.56	0.34	13.94	99.90		15	0.73	0.24
	48.94	0.19	32.38	0.88	0.26	2.13	0.25	14.84	99.87		30	0.78	0.20
	48.85	0.00	32.57	0.85	0.24	2.01	0.20	15.15	99.87		45	0.80	0.19
	51.43	0.26	30.74	0.86	0.20	2.92	0.32	13.13	99.86		55	0.70	0.28
	51.29	0.25	30.75	0.88	0.37	2.95	0.34	12.94	99.77		65	0.69	0.29
	51.31	0.28	30.69	0.84	0.30	3.05	0.36	13.03	99.86		75	0.69	0.29
	50.97	0.27	30.73	0.92	0.37	3.03	0.43	13.13	99.85		85	0.69	0.29
	50.25	0.32	30.99	0.97	0.44	3.11	0.39	13.32	99.79		95	0.69	0.29
	50.23	0.14	31.21	0.87	0.34	2.89	0.27	13.91	99.86		105	0.71	0.27
	50.50	0.16	31.34	0.83	0.24	2.78	0.23	13.80	99.88		115	0.72	0.26
	50.80	0.22	31.05	0.82	0.22	2.76	0.38	13.74	99.99		125	0.72	0.26
	51.51	0.20	30.44	0.84	0.30	3.09	0.42	13.09	99.89		135	0.68	0.29
	51.71	0.16	30.49	0.86	0.31	3.15	0.38	12.80	99.86		145	0.68	0.30
	51.28	0.19	30.73	0.78	0.23	3.04	0.36	13.27	99.88		155	0.69	0.29
	51.42	0.22	30.31	0.93	0.37	3.10	0.42	13.07	99.84		165	0.68	0.29
	51.10	0.23	30.64	0.88	0.29	3.04	0.42	13.24	99.84		175	0.69	0.29
	51.37	0.19	30.91	0.75	0.29	3.08	0.29	13.01	99.89		185	0.69	0.29
	51.46	0.25	30.49	0.86	0.39	3.24	0.42	12.74	99.85		195	0.67	0.31
	51.42	0.21	30.65	0.75	0.28	3.25	0.37	12.88	99.81		205	0.67	0.31
	49.87	0.08	31.91	0.77	0.32	2.42	0.29	14.29	99.95		215	0.75	0.23
	50.06	0.26	31.64	0.82	0.32	2.69	0.32	13.70	99.81		225	0.72	0.26
	51.19	0.17	30.94	0.85	0.34	3.18	0.38	12.87	99.92		235	0.67	0.30
	50.77	0.17	31.08	0.87	0.32	2.77	0.32	13.56	99.86		245	0.72	0.26
	49.99	0.19	31.62	0.86	0.27	2.46	0.40	14.00	99.79		255	0.74	0.24
	49.76	0.18	31.95	0.93	0.28	2.38	0.34	13.95	99.77		265	0.75	0.23
	49.42	0.13	32.26	0.78	0.25	2.23	0.28	14.50	99.85		275	0.77	0.21
	49.98	0.29	31.51	0.93	0.22	2.57	0.32	13.91	99.73		285	0.73	0.25
	51.57	0.11	30.62	0.88	0.36	3.21	0.38	12.78	99.91		315	0.67	0.31
	51.47	0.21	30.57	0.96	0.33	3.20	0.40	12.67	99.81		325	0.67	0.31
	53.00	0.26	29.50	0.85	0.48	3.67	0.52	11.59	99.87		335	0.61	0.35
	54.12	0.42	28.33	0.89	0.37	4.38	0.69	10.58	99.78	345 µm (rim)	0.55	0.41	0.04

TABLE 1 — *continued...*

2100 m	SiO ₂	TiO ₂	Al ₂ O ₃	FeO	MgO	CaO	Na ₂ O	K ₂ O	Total	An	Ab	Or
vent									0 µm (core)	0.56	0.40	0.03
	54.26	0.41	28.57	0.84	0.06	10.83	4.26	0.56	99.79			
	53.45	0.26	29.24	0.87	0.20	11.16	4.11	0.47	99.76	15	0.58	0.39
	51.52	0.18	30.70	1.13	0.21	12.76	3.03	0.37	99.90	40	0.68	0.29
	52.21	0.22	29.93	0.94	0.46	12.06	3.67	0.44	99.93	55	0.63	0.35
	51.23	0.10	31.04	1.02	0.20	12.86	3.08	0.31	99.84	70	0.68	0.30
	52.49	0.16	30.06	0.65	0.38	12.17	3.60	0.44	99.95	90	0.63	0.34
	52.49	0.22	29.93	0.85	0.33	11.98	3.57	0.40	99.77	110	0.63	0.34
	50.77	0.17	30.99	1.09	0.22	13.42	2.85	0.35	99.86	130	0.71	0.27
	50.11	0.18	31.64	0.87	0.28	13.93	2.57	0.24	99.82	160	0.74	0.25
	50.31	0.06	31.62	0.86	0.25	13.82	2.70	0.30	99.92	180	0.72	0.26
	49.89	0.18	31.70	0.94	0.29	13.91	2.70	0.26	99.87	200	0.73	0.26
	49.79	0.11	31.90	0.91	0.17	14.22	2.46	0.21	99.77	225	0.75	0.24
	49.64	0.19	31.75	0.97	0.32	14.08	2.62	0.28	99.85	240	0.74	0.25
	50.86	0.09	31.45	0.79	0.28	13.31	2.96	0.17	99.91	255	0.71	0.28
	50.39	0.18	31.27	0.88	0.21	13.69	2.89	0.31	99.82	270	0.71	0.27
	50.63	0.11	31.51	1.02	0.28	13.34	2.74	0.26	99.89	285	0.72	0.27
	49.41	0.18	32.08	0.90	0.25	14.32	2.39	0.32	99.85	300	0.75	0.23
	50.10	0.23	31.65	0.86	0.31	13.84	2.57	0.26	99.82	315	0.74	0.25
	50.01	0.24	31.60	0.92	0.24	13.70	2.72	0.31	99.74	330	0.72	0.26
	50.15	0.24	31.70	0.73	0.13	13.96	2.80	0.24	99.95	345	0.72	0.26
	50.20	0.18	31.68	0.74	0.31	13.92	2.61	0.26	99.90	365	0.73	0.25
	50.28	0.27	31.56	0.88	0.33	13.54	2.78	0.25	99.89	380	0.72	0.27
	50.90	0.16	31.29	0.77	0.31	13.38	2.80	0.28	99.89	395	0.71	0.27
	51.20	0.27	30.70	0.95	0.17	13.04	3.06	0.31	99.70	410	0.69	0.29
	52.43	0.24	29.92	0.98	0.29	11.81	3.78	0.42	99.87	425	0.62	0.36
	53.11	0.19	29.43	0.96	0.37	11.56	3.89	0.41	99.92	440	0.61	0.37
	53.06	0.23	29.32	0.92	0.35	11.61	3.93	0.46	99.88	455	0.60	0.37
	53.44	0.18	29.07	1.00	0.22	11.44	4.04	0.45	99.84	470	0.59	0.38
	63.03	0.46	21.36	1.11	0.24	3.40	6.42	3.85	99.87	485 µm (rim)	0.17	0.59

TABLE 1 — *continued...*

Laghetto	SiO ₂	TiO ₂	Al ₂ O ₃	FeO	MgO	CaO	Na ₂ O	K ₂ O	Total	0 μm (core)	An	Ab	Or	
vent	54.24	0.30	28.50	0.83	0.17	10.93	4.27	0.58	99.82		0.56	0.40	0.04	
	54.53	0.23	28.70	0.76	0.20	10.71	4.14	0.50	99.77		15	0.57	0.40	0.03
	53.73	0.29	29.01	0.85	0.29	11.09	4.15	0.47	99.88		30	0.58	0.39	0.03
	54.35	0.19	28.85	0.72	0.30	10.72	4.18	0.59	99.90		45	0.56	0.40	0.04
	53.94	0.31	28.97	0.75	0.28	10.73	4.30	0.53	99.81		60	0.56	0.41	0.03
	53.93	0.11	29.23	0.61	0.32	11.18	4.05	0.49	99.92		75	0.59	0.38	0.03
	53.66	0.25	28.98	0.78	0.40	11.22	4.09	0.52	99.90		90	0.58	0.38	0.03
	53.76	0.27	28.88	0.96	0.34	11.04	4.02	0.54	99.81		105	0.58	0.38	0.03
	54.03	0.24	28.96	0.75	0.18	11.07	4.17	0.52	99.92		120	0.58	0.39	0.03
	53.98	0.22	28.80	0.96	0.29	10.97	4.09	0.51	99.82		135	0.58	0.39	0.03
	53.90	0.22	29.14	0.64	0.27	11.08	4.12	0.53	99.90		150	0.58	0.39	0.03
	53.78	0.23	28.93	0.82	0.42	11.18	4.02	0.51	99.89		165	0.59	0.38	0.03
	54.18	0.24	28.73	0.89	0.16	11.01	4.15	0.42	99.78		180	0.58	0.39	0.03
	53.73	0.14	29.30	0.62	0.11	11.69	3.88	0.39	99.86		195	0.61	0.37	0.02
	54.19	0.23	28.95	0.75	0.15	10.87	4.23	0.55	99.92		210	0.57	0.40	0.03
	53.92	0.29	29.06	0.72	0.26	10.91	4.20	0.46	99.82		225	0.57	0.40	0.03
	53.57	0.26	29.19	0.78	0.33	11.16	4.09	0.44	99.82		240	0.58	0.39	0.03
	53.66	0.25	29.09	0.75	0.23	11.22	4.19	0.49	99.88		255	0.58	0.39	0.03
	53.38	0.30	29.20	0.92	0.34	10.99	4.12	0.52	99.77		270	0.58	0.39	0.03
	53.87	0.22	29.19	0.68	0.28	11.02	4.10	0.53	99.89		285	0.58	0.39	0.03
	53.72	0.22	29.27	0.81	0.17	11.02	4.08	0.52	99.81		300	0.58	0.39	0.03
	53.60	0.25	29.21	0.80	0.32	10.97	4.12	0.53	99.80		315	0.58	0.39	0.03
	54.56	0.19	28.42	0.78	0.23	10.61	4.40	0.60	99.79		330	0.55	0.41	0.04
	54.02	0.28	28.93	0.69	0.29	10.84	4.25	0.55	99.85		345	0.57	0.40	0.03
	54.05	0.21	29.01	0.80	0.22	10.93	4.10	0.54	99.86		360	0.58	0.39	0.03
	54.56	0.23	28.54	0.83	0.28	10.61	4.28	0.46	99.79		375	0.56	0.41	0.03
	54.05	0.29	28.63	0.74	0.30	11.02	4.32	0.56	99.91		390	0.57	0.40	0.03
	54.05	0.23	28.82	0.83	0.31	10.89	4.22	0.55	99.90		405	0.57	0.40	0.03
	54.04	0.24	29.13	0.76	0.25	10.81	4.16	0.49	99.88		420	0.57	0.40	0.03
	53.96	0.28	29.10	0.75	0.11	11.16	4.05	0.47	99.88		435	0.59	0.38	0.03
	54.17	0.22	28.86	0.77	0.23	10.84	4.15	0.56	99.80		450	0.57	0.39	0.04
	53.84	0.09	28.99	0.79	0.30	11.27	4.17	0.44	99.89		465	0.58	0.39	0.03
	54.82	0.29	28.16	0.79	0.11	10.79	4.37	0.59	99.92		480	0.56	0.41	0.04
	54.77	0.28	28.41	0.85	0.19	10.32	4.39	0.59	99.80		495	0.54	0.42	0.04
	53.03	0.30	29.47	0.82	0.36	11.51	3.88	0.45	99.82		510	0.60	0.37	0.03
	55.52	0.24	28.05	0.75	0.26	9.74	4.70	0.61	99.87		525	0.51	0.45	0.04
	54.82	0.30	28.20	0.89	0.35	10.09	4.55	0.62	99.82		540	0.53	0.43	0.04

TABLE 1 — *continued...*

Laghetto	SiO ₂	TiO ₂	Al ₂ O ₃	FeO	MgO	CaO	Na ₂ O	K ₂ O	Total	An	Ab	Or	
	52.95	0.33	29.50	0.90	0.33	11.58	3.82	0.47	99.88	555	0.61	0.36	0.03
	53.26	0.30	29.46	0.83	0.27	11.44	3.81	0.51	99.88	570	0.60	0.36	0.03
	54.19	0.16	28.91	0.76	0.25	10.96	4.07	0.57	99.87	585	0.58	0.39	0.04
	53.20	0.14	29.52	0.78	0.28	11.81	3.79	0.47	99.99	600	0.61	0.36	0.03
	52.56	0.25	29.72	1.02	0.20	11.92	3.66	0.54	99.87	615	0.62	0.35	0.03
	54.09	0.29	28.76	0.83	0.21	10.92	4.15	0.54	99.79	630	0.57	0.39	0.03
	53.78	0.22	29.12	0.86	0.25	11.10	3.93	0.57	99.83	645	0.59	0.38	0.04
	53.77	0.19	29.12	0.84	0.25	11.34	3.88	0.51	99.90	660	0.60	0.37	0.03
	53.04	0.32	29.40	0.89	0.37	11.36	3.88	0.51	99.77	675	0.60	0.37	0.03
	54.22	0.27	28.78	0.78	0.22	10.78	4.32	0.51	99.88	690	0.56	0.41	0.03
	54.88	0.20	28.48	0.81	0.19	10.43	4.23	0.58	99.80	705	0.56	0.41	0.04
	53.94	0.29	28.93	0.86	0.24	11.05	4.12	0.39	99.82	720	0.58	0.39	0.02
	55.09	0.16	28.26	0.75	0.30	10.20	4.42	0.67	99.85	735	0.54	0.42	0.04
	54.38	0.32	28.58	0.97	0.16	10.50	4.37	0.57	99.85	750	0.55	0.41	0.04
	54.60	0.38	28.23	0.92	0.26	10.55	4.32	0.59	99.85	765	0.55	0.41	0.04
	54.33	0.34	28.61	0.94	0.34	10.26	4.49	0.55	99.86	780	0.54	0.43	0.03
	50.23	0.24	31.25	0.87	0.31	13.94	2.72	0.26	99.82	795	0.73	0.26	0.02
	50.75	0.15	31.28	0.90	0.41	13.36	2.72	0.26	99.83	810	0.72	0.26	0.02
	50.52	0.14	31.31	0.86	0.34	13.67	2.93	0.21	99.98	825	0.71	0.28	0.01
	50.26	0.22	31.39	0.92	0.37	13.71	2.71	0.26	99.84	840	0.72	0.26	0.02
	50.12	0.17	31.49	0.80	0.32	14.07	2.63	0.22	99.82	855	0.74	0.25	0.01
	50.47	0.14	31.65	0.85	0.22	13.61	2.74	0.19	99.87	870	0.72	0.26	0.01
	50.08	0.19	31.49	0.91	0.30	13.65	2.85	0.32	99.79	885	0.71	0.27	0.02
	50.71	0.22	30.99	0.92	0.33	13.30	3.07	0.30	99.84	900	0.69	0.29	0.02
	51.27	0.08	30.67	0.95	0.36	13.02	3.17	0.33	99.85	915	0.68	0.30	0.02
	52.13	0.21	29.99	0.88	0.38	12.50	3.46	0.37	99.92	930	0.65	0.33	0.02
	52.13	0.26	29.85	1.01	0.29	12.23	3.58	0.41	99.76	945	0.64	0.34	0.03
	56.29	0.36	27.33	0.96	0.33	8.95	5.03	0.62	99.87	960 µm (rim)	0.48	0.48	0.04

al., 1981; Duncan and Preston, 1980), with their Mg# decreasing from core to rim (Fig. 2; Table 2).

More complex features have been observed in the products related to the N-S system. Lavas have oligophytic seriate texture with a P.I. ~10-20 and a mineral assemblage mainly composed of clinopyroxene (~10 vol.%) and subordinate plagioclase (~5 vol.%), Fo₇₉₋₇₀

olivine (<3 vol.%), Ti-magnetite (<3 vol.%). Mg-hastingsitic amphibole (~3 vol.%) and abundant quartzarenitic xenoliths (with mortar-texture) make these products peculiar (Clocchiatti *et al.*, 2004; Corsaro *et al.*, 2005; Viccaro *et al.*, 2006; 2007). Their groundmass is chiefly made up of plagioclase and clinopyroxene with olivine and Ti-magnetite as minor phases. As in the SE-PL products, plagioclase phenocrysts of the lavas

emitted from the lower end of this structure show a rather regular core-rim profile to decreasing An% contents (An_{75-55} ; Fig. 2; Table 1). On the other hand, plagioclase and clinopyroxene phenocrysts for the late-emitted volcanics at the higher end

(Laghetto vent) exhibit resorbed rims, enclosed by envelopes, with abruptly higher An% and Mg# values at their edges, which for plagioclase generally grade to Na-richer compositions toward the rim (Fig. 2; Table 1-2).

TABLE 2 — *Clinopyroxene compositions of representative phenocrysts in lavas of the 2001 eruption*

SE-PL	SiO ₂	TiO ₂	Al ₂ O ₃	Cr ₂ O ₃	FeO	MnO	MgO	CaO	Na ₂ O	K ₂ O	Total	Mg#	Wo	En	Fs		
vents	49.17	0.93	5.05	0.20	8.23	0.17	14.05	22.59	0.53	0.21	101.13	0 µm (core)	0.92	45.61	49.97	4.41	
	47.30	1.26	7.30	0.40	7.94	0.19	13.48	22.98	0.13	0.19	101.27		25	0.90	44.75	49.47	5.78
	46.59	1.34	8.05	0.29	8.41	0.09	12.98	22.92	0.00	0.19	100.86		50	0.87	44.33	47.58	8.09
	49.25	1.18	4.76	0.25	8.18	0.13	13.86	22.84	0.00	0.20	100.65		75	0.83	44.92	44.40	10.68
	48.15	1.36	5.54	0.20	8.99	0.18	13.13	22.24	0.00	0.14	99.93		100	0.79	43.91	42.17	13.92
	47.21	1.63	6.57	0.19	9.23	0.17	12.75	22.28	0.11	0.15	100.29		125	0.81	44.07	43.45	12.47
	44.77	2.32	9.39	0.13	10.18	0.20	11.64	22.01	0.00	0.18	100.82		150	0.79	42.52	42.70	14.78
	47.79	1.65	5.82	0.27	9.28	0.12	12.76	22.26	0.31	0.21	100.85		175	0.82	44.94	43.70	11.36
	47.54	1.41	6.26	0.13	9.91	0.22	13.10	22.11	0.27	0.14	101.09		200	0.84	43.60	46.33	10.07
	49.45	1.01	4.27	0.22	8.59	0.26	14.41	21.98	0.03	0.19	100.48		225	0.84	43.05	46.46	10.49
	48.57	1.48	4.89	0.00	8.42	0.18	13.50	22.15	0.45	0.05	99.69		250	0.84	45.16	44.92	9.92
	49.48	1.47	4.38	0.03	8.92	0.18	13.45	22.08	0.51	0.00	100.51		300	0.81	44.97	42.53	12.50
	48.02	1.88	5.67	0.00	9.28	0.26	12.86	21.40	0.56	0.00	99.93		325	0.79	43.83	42.31	13.86
	49.42	1.50	4.96	0.00	8.65	0.26	13.80	21.52	0.50	0.00	100.61		350	0.81	43.42	44.06	12.52
	48.93	1.55	5.14	0.03	8.24	0.17	13.54	22.17	0.38	0.00	100.15		375	0.82	44.69	43.31	12.00
	49.19	1.86	4.86	0.01	8.21	0.28	13.22	22.27	0.59	0.01	100.49		400	0.81	45.69	42.27	12.04
	47.83	2.10	5.77	0.02	8.76	0.25	12.60	22.19	0.58	0.00	100.10	425 µm (rim)	0.81	45.70	41.99	12.31	

2100 m	SiO ₂	TiO ₂	Al ₂ O ₃	Cr ₂ O ₃	FeO	MnO	MgO	CaO	Na ₂ O	K ₂ O	Total	Mg#	Wo	En	Fs		
vent	49.55	1.18	4.46	0.15	8.24	0.19	14.28	22.21	0.00	0.13	100.39	0 µm (core)	0.82	43.51	44.54	11.95	
	49.66	1.27	4.61	0.19	7.88	0.14	13.90	22.00	0.10	0.20	99.95		25	0.80	43.87	43.03	13.10
	49.29	1.56	5.68	0.17	8.69	0.17	13.16	22.35	0.00	0.20	101.27		50	0.77	43.79	39.93	16.28
	46.33	1.98	7.47	0.14	9.49	0.18	12.21	22.27	0.36	0.19	100.62		75	0.84	44.81	44.94	10.24
	48.87	1.17	5.35	0.31	8.44	0.17	13.56	22.34	0.28	0.17	100.66		100	0.84	44.58	45.53	9.89
	48.25	1.46	5.16	0.19	8.94	0.25	12.96	22.20	0.00	0.22	99.63		125	0.79	44.29	41.39	14.32
	51.25	0.95	2.69	0.22	8.79	0.30	14.44	22.04	0.23	0.21	101.28		150	0.82	44.03	43.79	12.18
	49.04	1.50	4.91	0.29	9.45	0.24	12.80	22.17	0.29	0.23	100.92		175	0.79	44.73	41.02	14.25
	48.83	1.29	4.75	0.27	9.15	0.25	13.38	22.04	0.05	0.21	100.22		200	0.80	43.71	42.73	13.57
	50.29	1.10	3.00	0.27	8.90	0.19	14.31	21.99	0.03	0.16	100.25	225 µm (rim)	0.80	43.63	42.90	13.47	

TABLE 2 — *continued...*

Laghetto	SiO ₂	TiO ₂	Al ₂ O ₃	Cr ₂ O ₃	FeO	MnO	MgO	CaO	Na ₂ O	K ₂ O	Total	Mg#	Wo	En	Fs		
vent	48.57	1.48	4.89	0.00	8.42	0.18	13.50	22.15	0.45	0.05	99.69	0 µm (core)	0.84	45.16	44.92	9.92	
	49.48	1.47	4.38	0.03	8.92	0.18	13.45	22.08	0.51	0.00	100.51		25	0.81	44.97	42.53	12.50
	48.02	1.88	5.67	0.00	9.28	0.26	12.86	21.40	0.56	0.00	99.93		50	0.79	43.83	42.31	13.86
	48.65	1.57	5.61	0.06	8.07	0.21	13.60	22.35	0.42	0.00	100.53		75	0.84	44.87	45.09	10.05
	49.28	1.58	4.70	0.05	8.49	0.26	13.53	22.64	0.51	0.00	101.04		100	0.84	45.81	44.09	10.10
	49.23	1.41	4.37	0.03	8.86	0.15	13.56	22.12	0.55	0.00	100.28		125	0.83	45.20	44.01	10.80
	49.89	1.42	4.03	0.00	8.77	0.26	13.95	22.09	0.49	0.00	100.89		150	0.83	44.61	44.10	11.29
	49.42	1.50	4.96	0.00	8.65	0.26	13.80	21.52	0.50	0.00	100.61		175	0.81	43.42	44.06	12.52
	48.93	1.55	5.14	0.03	8.24	0.17	13.54	22.17	0.38	0.00	100.15		200	0.82	44.69	43.31	12.00
	49.19	1.86	4.86	0.01	8.21	0.28	13.22	22.27	0.59	0.01	100.49		225	0.81	45.69	42.27	12.04
	47.83	2.10	5.77	0.02	8.76	0.25	12.60	22.19	0.58	0.00	100.10		250	0.81	45.70	41.99	12.31
	46.94	2.69	6.43	0.00	9.61	0.08	12.09	21.94	0.38	0.03	100.17		275	0.76	44.73	38.31	16.97
	49.69	1.52	4.21	0.05	8.93	0.22	13.58	21.67	0.51	0.01	100.39		300	0.80	44.19	42.19	13.62
	49.81	1.58	4.10	0.06	8.65	0.31	13.52	21.91	0.47	0.01	100.43		325	0.79	44.59	41.46	13.95
	50.47	1.56	4.30	0.05	8.94	0.25	13.46	21.59	0.52	0.03	101.18		350	0.77	43.83	39.94	16.24
	48.83	1.51	4.99	0.00	8.36	0.23	13.74	22.31	0.47	0.00	100.43		375	0.85	45.04	45.59	9.36
	48.91	1.52	5.01	0.00	7.63	0.17	13.69	22.54	0.48	0.00	99.95		400	0.85	45.86	45.06	9.08
	48.25	1.74	5.83	0.00	8.26	0.22	13.46	22.58	0.46	0.00	100.80		425	0.86	45.38	45.76	8.87
	49.39	1.22	4.54	0.00	7.93	0.13	13.87	22.43	0.38	0.00	99.89	450 µm (rim)	0.84	45.33	44.36	10.31	

WHOLE ROCK COMPOSITIONS

The 2001 eruption volcanics plot in the trachybasaltic field of the TAS diagram, with a mildly potassic character, and may be defined as K-trachybasalt ($\text{Na}_2\text{O} - 2 \leq \text{K}_2\text{O}$; Le Maitre, 2002). Their petrochemical features fit the main trend observed after the 1971 eruption at Mt. Etna, as they also are characterised by a LILE enrichment and a decrease in some incompatible elements, particularly Th (Armienti *et al.*, 1989; Condomines *et al.*, 1995; Tonarini *et al.*, 2001; Tanguy *et al.*, 1997; Viccaro and Cristofolini, 2008). A careful examination of the sampled products has pointed out significant changes of whole rock compositions (Fig. 3; Table 3). Specifically, SE-PL lavas are quite similar to the recent products of the summit craters (Corsaro and Pompilio, 2004), being their

variability chiefly ascribed to differentiation within the magma column in the steadily degassing open-conduit. On the other hand, lavas erupted from the N-S fracture system show a more complex space- and time-related variability. Products early-erupted at 2100 m are slightly more evolved in their compositions, compared to the late-erupted ones at the higher Laghetto vent, which are slightly more primitive and characterized by a distinct trace element signature (Fig. 3; cf. Viccaro *et al.*, 2006; Ferlito *et al.*, 2008a; Viccaro and Cristofolini, 2008).

Concerning their radiogenic isotope signature, all of the analyzed products display values well in the range recognized for the recent Etnean ones (cf. Viccaro and Cristofolini, 2008). SE-PL lavas are similar to the ones from the lower section of the N-S structure (2100 m vent), whereas the late-

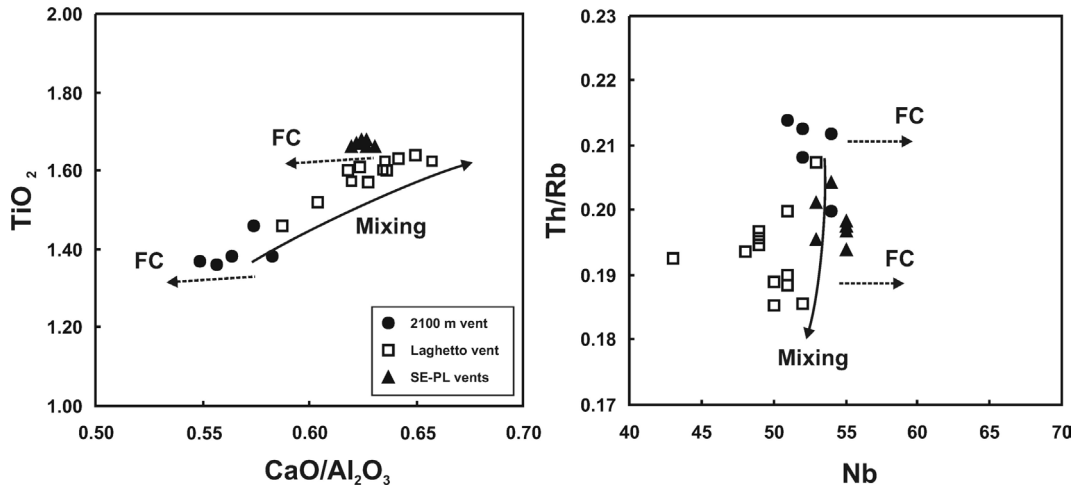


Fig. 3 – $\text{CaO}/\text{Al}_2\text{O}_3$ vs. TiO_2 and Nb vs. Th/Rb variation diagrams for lavas of the 2001 eruption. The solid line arrow indicates a mixing between the products emitted at the 2100 m vent and an inferred more primitive magma. Simulations of differentiation for major elements (dashed arrows) via fractional crystallization (FC) were performed using MELTS (Ghiorso and Sack, 1995; Asimow and Ghiorso, 1998). FC for the products emitted at 2100 m was simulated taking into account the most basic whole rock compositions erupted at the vent with $T = 990^\circ\text{C}$, $P = 250 \text{ MPa}$ and $f\text{O}_2$ at the QFM buffer [cf. Viccaro *et al.* (2006) and Ferlito *et al.* (2008a) for the choice of physical parameters]. The H_2O content was assumed as 2.5 wt.% on the basis of H_2O values generally acknowledged for similar Etnan magmas (Métrich and Rutherford, 1998). Under these conditions, the computed stable mineral assemblage is composed of ~58 vol.% of liquid, ~25 vol.% of clinopyroxene, ~10 vol.% of plagioclase (An_{71}), ~4 vol.% of magnetite, ~3 vol.% olivine (Fo_{72}) and trace of apatite. Mg-hastingsite was not included in the simulation, due to the poor reliability of MELTS in dealing with hydrous phases. FC within the open-conduit for the SE-PL products was simulated considering the most basic SE-PL whole rock composition at $T = 1100^\circ\text{C}$, $P = 50 \text{ MPa}$ and $f\text{O}_2$ at the QFM buffer. The H_2O content was assumed as 2.5 wt%, in accordance with Métrich and Rutherford (1998). Results show that, after crystallization of olivine (~3 vol.%) and clinopyroxene (~11 vol.%) at depth, the FC trend at shallow depth (~1.5 km) is mainly controlled by plagioclase (~20 vol.%) plus magnetite (~3 vol.%), leading to a final total volume of ~37% of solid phases fractionated.

emitted lavas from the Laghetto vent (2550 m a.s.l.) are markedly different, as they display higher Sr and lower Nd and Pb ratios (Table 4).

Finally, distinct $\delta^{18}\text{O}$ values have been observed during the 2001 eruption: lavas from the SE-PL and Laghetto vents exhibit similar $\delta^{18}\text{O}$ values (mean +6.2‰), whereas they increase up to around +7.1‰ in products of the vent system at 2100 m (Table 4).

RESIDUAL GLASSES IN TEPHRA GRAINS

The most important changes of petrographic and geochemical features of the products and of eruptive styles certainly occurred at the vents of the N-S eruptive structure. For these reasons,

attention was also paid to the tephra ejected from: i) the 2100 m vent (Calcarazzi area) in the first eruptive phase and ii) at the Laghetto vent (2550 m a.s.l.), from the middle and top levels of the cinder cone, which represent its intermediate and final stages of activity. The sideromelane glass appears as residual with respect to the related lavas, as it is trachyandesitic in tephra of the 2100 m vent, whereas it ranges from trachyandesitic to phonotephritic (Table 5) in the middle and top levels of the Laghetto sequence. Major element concentrations are rather uniform, except little differences for TiO_2 , FeO and P_2O_5 , which are lower in the tephra from the vent at 2100 m and moderately increase from the middle to the top levels of the Laghetto sequence (Table 5). The most important variation of the residual glass compositions regards their

TABLE 3 — Major and trace element concentrations for lavas of the 2001 eruption (data from supplementary on-line material in Viccaro and Cristofolini, 2008)

Sample	CAL1	CAL2	CAL3	CAL4	CAL5	LAG6	LAG7	LAG8	LAG9	LAG10	LAG11	LAG12	LAG13
Vent	2100 m	Laghetto											
Lat	37° 42'	37° 42'	37° 42'	37° 42'	37° 41'	37° 43'	37° 43'	37° 43'	37° 43'	37° 43'	37° 43'	37° 43'	37° 43'
	19.63°N	15.06°N	6.36°N	1.16°N	58.95°N	8.53°N	7.49°N	5.92°N	5.00°N	12.38°N	12.90°N	3.24°N	2.61°N
Lon	15° 0'	15° 0'	15° 0'	15° 0'	15° 0'	15° 0'	15° 0'	15° 0'	15° 0'	15° 0'	15° 0'	15° 0'	15° 0'
	21.16°E	18.02°E	9.93°E	9.97°E	9.53°E	4.96°E	4.41°E	3.54°E	2.82°E	21.39°E	20.77°E	1.55°E	0.91°E
SiO ₂	48.26	48.46	48.41	48.54	48.67	47.35	47.38	47.66	47.52	47.62	47.40	47.46	47.41
TiO ₂	1.46	1.38	1.38	1.37	1.36	1.60	1.57	1.63	1.52	1.46	1.64	1.61	1.60
Al ₂ O ₃	17.92	17.94	18.20	18.34	18.28	17.82	17.43	17.40	17.85	18.15	17.26	17.42	17.39
Fe ₂ O ₃	5.79	3.58	3.25	3.33	2.74	4.90	5.83	4.23	4.54	3.73	4.90	4.26	5.81
FeO	3.95	5.62	5.79	5.65	6.18	5.64	4.87	6.45	5.34	5.84	5.92	6.09	4.87
FeO _{tot}	9.16	8.84	8.72	8.65	8.65	10.05	10.12	10.26	9.43	9.20	10.33	9.92	10.10
MgO	5.63	5.70	5.65	5.67	5.61	5.75	6.16	5.58	5.84	5.69	5.92	5.83	5.75
MnO	0.17	0.17	0.16	0.16	0.16	0.18	0.18	0.19	0.17	0.17	0.19	0.18	0.19
CaO	10.28	10.45	10.26	10.07	10.17	11.02	10.94	11.16	10.78	10.66	11.21	10.86	11.06
Na ₂ O	3.98	4.12	4.31	4.26	4.21	3.40	3.33	3.30	3.96	4.09	3.22	3.77	3.50
K ₂ O	2.03	2.04	2.07	2.07	2.07	1.91	1.84	1.95	1.98	2.05	1.94	2.02	1.95
P ₂ O ₅	0.53	0.53	0.53	0.53	0.53	0.44	0.46	0.44	0.50	0.53	0.41	0.50	0.46
L.O.I.	0.58	0.37	0.31	0.34	0.29	0.48	0.59	0.43	0.45	0.38	0.48	0.43	0.59
Rb	46.1	47.2	44.9	46.1	48.0	46.6	44.2	46.3	47.5	49.3	48.3	45.5	46.2
Sr	1110	1140	1080	1120	1150	1120	1160	1140	1130	1160	1120	1110	1130
Y	29.5	30.0	28.6	29.5	30.4	30.0	30.0	29.7	29.7	31.4	30.5	30.1	30.1
Zr	199	203	193	194	203	187	188	196	193	201	195	190	188
Nb	52	54	51	52	54	50	49	53	50	43	51	51	49
Ba	608	632	593	601	623	589	571	616	589	626	612	585	585
La	65.4	70.1	65.5	66.3	67.1	62.1	62.2	66.8	63.0	66.5	64.9	64.5	62.4
Ce	123	132	124	124	126	118	118	125	119	126	123	123	120
Pr	13.0	14.1	13.1	13.1	13.6	12.6	12.7	13.5	12.6	13.6	13.1	13.4	12.9
Nd	56.4	60.6	56.2	56.6	58.0	54.6	56.6	57.6	54.0	58.4	56.1	57.3	56.3
Sm	10.0	10.6	9.5	9.7	10.1	9.5	9.9	10.1	9.8	10.3	10.0	10.4	10.0
Eu	2.64	2.98	2.76	2.81	2.91	2.67	2.85	2.89	2.76	2.95	2.83	2.81	2.79
Gd	9.09	9.95	9.10	8.92	9.37	9.16	9.21	9.29	9.33	9.57	9.42	9.28	9.01
Tb	1.29	1.37	1.3	1.29	1.34	1.32	1.29	1.31	1.31	1.36	1.31	1.33	1.3
Dy	6.33	6.53	6.31	6.37	6.29	6.14	6.67	6.49	6.37	6.73	6.39	6.41	6.23

TABLE 3 — *continued...*

Sample	CAL1	CAL2	CAL3	CAL4	CAL5	LAG6	LAG7	LAG8	LAG9	LAG10	LAG11	LAG12	LAG13
Vent	2100 m	Laghetto											
	37° 42'	37° 42'	37° 42'	37° 42'	37° 41'	37° 43'	37° 43'	37° 43'	37° 43'	37° 43'	37° 43'	37° 43'	37° 43'
Lat	19.63°N	15.06°N	6.36°N	1.16°N	58.95°N	8.53°N	7.49°N	5.92°N	5.00°N	12.38°N	12.90°N	3.24°N	2.61°N
	15° 0'	15° 0'	15° 0'	15° 0'	15° 0'	15° 0'	15° 0'	15° 0'	15° 0'	15° 0'	15° 0'	15° 0'	15° 0'
Lon	21.16°E	18.02°E	9.93°E	9.97°E	9.53°E	4.96°E	4.41°E	3.54°E	2.82°E	21.39°E	20.77°E	1.55°E	0.91°E
Ho	1.16	1.27	1.16	1.22	1.23	1.17	1.15	1.22	1.20	1.24	1.21	1.22	1.16
Er	2.95	3.30	2.88	2.94	3.13	3.15	3.06	3.29	3.12	3.14	3.10	3.26	3.06
Tm	0.38	0.40	0.36	0.37	0.38	0.35	0.37	0.38	0.37	0.41	0.39	0.40	0.38
Yb	2.3	2.5	2.4	2.5	2.5	2.4	2.5	2.5	2.5	2.5	2.5	2.6	2.4
Lu	0.36	0.40	0.37	0.37	0.40	0.37	0.36	0.39	0.37	0.38	0.37	0.39	0.36
Hf	5	5	5	5	5	5	5	5	5	5	5	5	5
Ta	2.4	2.5	2.4	2.4	2.5	2.2	2.2	2.5	2.3	2.3	2.4	2.4	2.3
Pb	5	5	5	5	5	5	5	5	5	5	5	5	5
Th	9.6	10.0	9.6	9.8	9.6	8.8	8.7	9.6	8.8	9.5	9.1	9.1	9.0
U	2.71	2.83	2.69	2.77	2.82	2.55	2.53	2.69	2.50	2.65	2.65	2.69	2.59
Sc	26	28	27	26	26	27	27	27	29	27	28	29	28
V	282	294	272	285	294	295	304	286	296	310	308	304	294
Cr	38	45	37	42	35	37	48	41	40	40	42	36	36
Co	35.3	36.4	33.5	34.9	36.7	37.1	39.0	35.0	36.9	37.8	38.3	36.6	35.5
Ni	32	34	28	32	32	32	38	28	34	40	34	31	32

K_2O and chlorine contents, that may be related to the vent location and to the timing of the eruptive activity, and are highest in the uppermost tephra levels of the Laghetto cone (Fig. 4; cf. Ferlito *et al.*, 2008a).

DISCUSSION AND CONCLUSIONS

All of the available petrographic and geochemical data show that three different magmas took part in the distinct phases of the 2001 eruption on the southern flank of Mt. Etna. In particular, the magma, erupted through NNW-SSE trending structures at the South East crater and Piano del Lago vents (SE-PL system) was a plagioclase-rich trachybasalt, whereas the one erupted first

through N-S trending fractures at the 2100 m vent was amphibole-bearing trachybasaltic, and rose up from a ~6 km deep eccentric closed reservoir (Viccaro *et al.*, 2007). In the meantime, the two tectonic systems extended and intersected in the Laghetto area (2550 m; Fig. 1) just few days after the eruption onset (Monaco *et al.*, 2005). Here, a different magma was erupted from a new vent, with compositional features not consistent with differentiation by fractional crystallization of either of the SE-PL and 2100 m vent ones, as indicated by both a MELTS simulation of a fractionation process for major elements and the trace element ratios variability (Fig. 3). We interpret the composition of lavas erupted at the Laghetto vent as the result of mixing between the amphibole-bearing trachybasalt and a deep, more

TABLE 3 — *continued...*

Sample	LAG14	LAG15	LAG16	LAG17	SE-PL1	SE-PL2	SE-PL4	SE-PL5	SE-PL6	SE-PL7	SE-PL8	SE-PL9
Vent	Laghetto	Laghetto	Laghetto	Laghetto	SE-PL							
	37° 43'	37° 43'	37° 43'	37° 43'	37° 43'	37° 43'	37° 43'	37° 44'	37° 43'	37° 44'	37° 44'	37° 44'
Lat	9.65°N	9.03°N	14.33°N	13.72°N	55.49°N	52.28°N	41.68°N	30.31°N	42.27°N	29.19N	30.23°N	30.31°N
	15° 0'	15° 0'	15° 0'	15° 0'	15° 0'	15° 0'	15° 0'	15° 0'	15° 0'	15° 0'	15° 0'	15° 0'
Lon	5.60°E	4.66°E	9.32°E	9.17°E	14.48°E	15.12°E	15.19°E	1.73°E	12.35°E	2.68°E	1.77°E	2.41°E
SiO ₂	47.53	47.54	47.15	47.06	47.38	47.40	47.39	47.42	47.43	47.46	47.44	47.45
TiO ₂	1.58	1.60	1.62	1.62	1.66	1.67	1.67	1.68	1.66	1.67	1.66	1.68
Al ₂ O ₃	17.53	17.27	17.31	17.14	17.84	17.81	17.82	17.80	17.70	17.75	17.78	17.83
Fe ₂ O ₃	4.50	5.40	5.03	5.15	4.21	4.24	4.18	4.88	5.27	4.28	4.48	4.62
FeO	5.83	5.23	5.81	5.96	6.53	6.54	6.59	5.92	5.58	6.48	6.33	6.25
FeO _{tot}	9.88	10.09	10.34	10.60	10.32	10.36	10.35	10.31	10.32	10.33	10.36	10.41
MgO	5.83	5.99	5.99	6.44	5.34	5.27	5.30	5.29	5.32	5.28	5.26	5.33
MnO	0.18	0.19	0.19	0.19	0.19	0.19	0.19	0.19	0.19	0.19	0.19	0.19
CaO	10.94	10.98	11.30	10.91	11.05	11.15	11.09	11.12	11.17	11.10	11.14	11.18
Na ₂ O	3.63	3.42	3.27	3.22	3.34	3.31	3.32	3.30	3.29	3.33	3.27	3.30
K ₂ O	1.98	1.95	1.85	1.89	2.02	1.99	2.01	1.99	2.02	2.00	1.99	2.00
P ₂ O ₅	0.46	0.44	0.47	0.43	0.44	0.44	0.44	0.44	0.44	0.44	0.44	0.44
L.O.I.	0.46	0.53	0.51	0.51	0.42	0.41	0.42	0.46	0.46	0.45	0.47	0.19
Rb	47.4	50.1	44.9	45.5	46.2	49.1	46.5	48.8	47.4	46.7	49.0	47.6
Sr	1120	1160	1130	1080	1170	1220	1180	1210	1170	1190	1200	1160
Y	30.2	31.4	29.7	29.4	30.4	31.8	30.4	31.8	30.5	30.4	31.8	30.5
Zr	194	197	185	186	198	204	200	202	205	201	206	205
Nb	51	52	48	49	53	55	54	55	55	53	55	53
Ba	606	622	560	571	641	661	645	665	640	650	660	643
La	64.9	66.4	61.7	61.6	66.6	68.9	67.1	68.5	66.2	66.8	68.1	66.4
Ce	121	125	118	116	126	129	128	131	127	125	130	122
Pr	13.2	13.6	12.7	12.6	13.5	13.8	13.6	13.7	13.5	13.7	13.8	13.6
Nd	56.1	58.5	56.1	54.0	57.1	59.3	57.9	59.0	57.7	57.5	58.8	57.4
Sm	10.3	10.6	10.0	9.5	10.3	10.5	10.2	10.4	10.3	10.5	10.4	10.1
Eu	2.81	2.94	2.83	2.76	2.86	3.01	2.84	2.99	2.81	2.88	3.03	2.85
Gd	9.17	9.46	9.08	9.01	9.33	9.69	9.36	9.62	9.27	9.38	9.58	9.26
Tb	1.31	1.36	1.32	1.27	1.3	1.4	1.3	1.4	1.3	1.3	1.4	1.3
Dy	6.62	6.64	6.44	6.08	6.46	6.69	6.44	6.67	6.29	6.48	6.70	6.33
Ho	1.21	1.19	1.21	1.17	1.19	1.24	1.19	1.23	1.22	1.20	1.21	1.21
Er	3.00	3.20	3.06	2.94	3.11	3.27	3.13	3.28	3.18	3.09	3.25	3.13
Tm	0.38	0.40	0.36	0.36	0.37	0.40	0.38	0.39	0.39	0.37	0.39	0.40
Yb	2.4	2.6	2.5	2.3	2.5	2.6	2.6	2.4	2.5	2.4	2.6	2.5

TABLE 3 — *continued...*

Sample	LAG14	LAG15	LAG16	LAG17	SE-PL1	SE-PL2	SE-PL4	SE-PL5	SE-PL6	SE-PL7	SE-PL8	SE-PL9
Vent	Laghetto	Laghetto	Laghetto	Laghetto	SE-PL							
	37° 43'	37° 43'	37° 43'	37° 43'	37° 43'	37° 43'	37° 43'	37° 44'	37° 43'	37° 44'	37° 44'	37° 44'
Lat	9.65°N	9.03°N	14.33°N	13.72°N	55.49°N	52.28°N	41.68°N	30.31°N	42.27°N	29.19N	30.23°N	30.31°N
	15° 0'	15° 0'	15° 0'	15° 0'	15° 0'	15° 0'	15° 0'	15° 0'	15° 0'	15° 0'	15° 0'	15° 0'
Lon	5.60°E	4.66°E	9.32°E	9.17°E	14.48°E	15.12°E	15.19°E	1.73°E	12.35°E	2.68°E	1.77°E	2.41°E
Lu	0.36	0.40	0.37	0.36	0.36	0.39	0.37	0.36	0.37	0.37	0.36	0.39
Hf	5	5	5	5	5	5	5	5	5	5	5	5
Ta	2.3	2.4	2.1	2.3	2.4	2.6	2.4	2.5	2.4	2.5	2.6	2.4
Pb	5	5	5	5	5	5	5	5	5	5	5	5
Th	9.0	9.3	8.7	8.9	9.3	9.7	9.5	9.6	9.4	9.4	9.5	9.3
U	2.59	2.70	2.51	2.51	2.69	2.83	2.78	2.80	2.76	2.72	2.74	2.70
Sc	28	28	28	28	25	25	25	25	25	25	25	25
V	297	312	307	291	291	303	294	301	295	292	300	296
Cr	40	36	37	36	28	20	26	22	23	25	24	21
Co	36.3	38.7	36.7	39.5	34.6	35.1	34.8	34.9	34.4	34.7	35.2	34.6
Ni	33	36	37	42	33	28	31	29	27	30	32	26

primitive end member, not erupted as such during the 2001 event. This doesn't contrast with the hypothesis of Corsaro *et al.* (2007), who correctly ruled out mixing between magmas erupted from the different systems SE-PL and N-S-oriented, but they didn't explain why a hotter, more primitive and undegassed magma was erupted just at the Laghetto. In addition, evidence for a more primitive, volatile-rich magma was also found by Métrich *et al.* (2004) as melt inclusions in olivine phenocrysts of lavas erupted at the Laghetto vent. This end-member has been progressively involved in the recent Etnan activity, and finally reached the main conduit of the persistently active summit craters during the interval between the 2002-03 and 2004-05 eruptions (Viccaro and Cristofolini, 2008; Ferlito *et al.*, 2008b).

Little-scale oscillatory zoning has been ascribed to local changes in growth-kinetics at the crystal-melt interface, without necessarily implying significant variations of physical-chemical conditions of the magmatic systems (Allegre *et al.*, 1981; Cashman, 1990; Ortoleva, 1990; L'Heureux, 1993; Holten *et al.*, 2000). This may be considered as the main process controlling the phenocrysts evolution in lavas emitted from the

open summit vents. Here, magma differentiation is chiefly driven by polybaric crystallization, related to convectional movements within the steadily degassing open-conduit, and fractionation effects are continuously buffered by new magma inputs. According to this model, large plagioclase and clinopyroxene phenocrysts in the SE-PL volcanics do not show significant changes in their An% and Mg# respectively, a feature consistent with the growth in such a dynamic system (Fig. 2). Although lavas emitted from the 2100 m vents are certainly unrelated to the open-conduit as proved by the Mg-hastingsite occurrence, which suggests crystallization in a closed magma reservoir (cf. Viccaro *et al.*, 2007), the plagioclase and clinopyroxene phenocrysts in these lavas are rather homogeneous in their features (Fig. 2). On the contrary, phenocryst textures and chemistry of products emitted at the Laghetto vent markedly differ from those of the SE-PL and 2100 m vents. Specifically, abrupt changes towards high An% and Mg# for plagioclase and clinopyroxene respectively have been recognized next to their rims, often associated to highly developed sieve textures in plagioclase (Fig. 2). In order to verify if these features are a record of magma

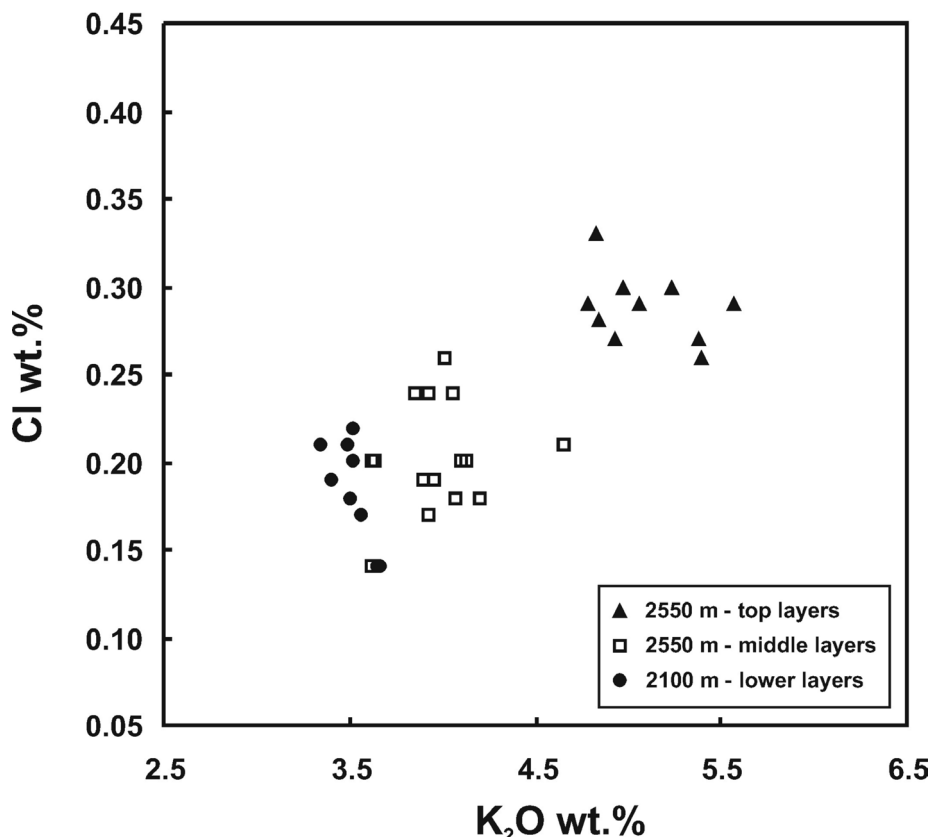


Fig. 4 – K₂O vs. Cl diagram (wt.%) for residual glass compositions in tephra grains erupted at the 2100 m and Laghetto vents. The positive correlation between Cl and K, both of which increase towards the middle and top layers of the Laghetto sequence, indicates the role played by volatiles in carrying Cl-complexes of K (and Ti, Fe, P, not shown).

mixing, the distribution coefficients of Ca/Na (for plagioclase) and Fe/Mg (for clinopyroxene) were considered to test if rims of plagioclase and clinopyroxene grew in equilibrium with the hosting melt. The composition of the less evolved lava erupted at the Laghetto vent, characterized by the lowest porphyritic index, has been assumed as representative of the magma composition. $\text{Ca}^{/\text{Na}} D_{\text{plg}/\text{melt}}$ of plagioclase ranging between 1.7 and 5.5 were considered, corresponding to equilibrium conditions with basaltic melts at 200 MPa and H₂O contents between 2 and 6 wt% (Sisson and Groove, 1993). In spite of the uncertainty for $\text{Ca}^{/\text{Na}} D_{\text{plg}/\text{melt}}$ values, envelopes affected by resorption at the rim of phenocrysts generally appear as far away from equilibrium conditions (Fig. 2). Expected

equilibrium conditions between melt and rims of the hosted clinopyroxene have been calculated on the basis of $\text{Fe}^{/\text{Mg}} D_{\text{cpx}/\text{melt}} = 0.23\text{--}0.30$ (Sisson and Groove, 1993). Results show that lava and hosted clinopyroxene phenocrysts often are not under equilibrium (Fig. 2). In particular, crystals rims are less evolved (higher Mg# values) than expected according to the calculated theoretical equilibrium. This evidence further supports the idea that the observed variability of the Laghetto volcanics could derive from a mixing with a more primitive magma occurred slightly before the eruption.

Further indications are supplied by the radiogenic and stable isotope geochemistry. Lavas erupted at the Laghetto vent tend to higher Sr and lower Nd-Pb radiogenic values, displaying a signature

markedly distinct from that of the products emitted at the 2100 m and SE-PL vents, as well as from the general trend developed after the 1971 eruption (Armienti *et al.*, 1989; Barbieri *et al.*, 1993; Tanguy *et al.*, 1997; Tonarini *et al.*, 2001; Viccaro and Cristofolini, 2008). Such an isotopic diversity indicates that the more primitive magma involved in the mixing was also isotopically distinct, which makes the 2001 event a benchmark in the recent petrological evolution of Etnean magmas.

Other hints for clarifying various aspects of magma evolution during its residence in a crustal reservoir could derive by considering the observed $\delta^{18}\text{O}$ variability. Volcanics erupted at the 2100 m vent exhibit higher $\delta^{18}\text{O}$ values than the ones emitted at the Laghetto and SE-PL vents. It is worth reminding that lavas emitted by the 2100 m vent display the peculiar and uncommon amphibole occurrence joined to exceptionally large amounts of quartzarenitic xenoliths (whose measured $\delta^{18}\text{O}$ is +12.7‰; Table 4). Amphibole crystallization may be made possible due to the storage of magma in a closed chamber for time long enough to attain the required volatile pressure (Viccaro *et al.*, 2007). The Sr-Nd-Pb-O isotopic variability recognized in recent Etnean magmas scarcely depends on contamination induced by the sedimentary basement underlying the volcanic edifice (Viccaro and Cristofolini, 2008). Conversely, it has been strictly related to varying degrees of metasomatic modifications at the source, where the contribution of fluids and/or

silicate melts somehow related to a hydrothermally altered lower oceanic crust increased through time. However, the higher $\delta^{18}\text{O}$ value exclusive of products erupted at the 2100 m vent, not associated to variations towards significantly higher Sr and lower Nd-Pb, may be attributed to contamination by the sedimentary basement. These contrasting features of the erupted volcanics suggest that this process may be important at Mt. Etna under peculiar conditions in the feeding system, namely when magma resides in closed reservoirs for long time.

Evidence for other processes, which acted on the magma erupted by the Laghetto vent, is derived from microanalysis of residual glasses in tephra collected at the vent: these data suggest that usual differentiation processes (e.g., fractional crystallization or mixing with a more primitive magma) are inadequate for interpreting their time-related anomalous enrichment in Ti, Fe, P, K and Cl. These data support a model of mobile element transfer depending on the diffusion of fluids from the primitive, volatile-rich magma into the amphibole-bearing trachybasalt, through fracture networks probably activated during the seismic crisis of April 2001 (Patanè *et al.*, 2002; Fig. 5). Assuming the intruding, isotopically distinct magma as the primitive component found in olivine phenocrysts by Métrich *et al.* (2004), information on its volatile composition might be also obtained: specifically, these authors highlighted that the total amount of volatile species (H_2O , CO_2 , Cl, S,

TABLE 4 — *Sr - Nd - Pb* and *O* isotope compositions of selected Etnean lavas of the 2001 eruption; a $\delta^{18}\text{O}$ value for a Numidian Flysch quartzarenite (QZ-FN) has been reported (data from Viccaro and Cristofolini, 2008)

F) in the inclusions is up to about 4 wt.%, rather uncommon for trachybasaltic compositions. Thermodynamic simulations for constraining the volatile saturation pressure for magmas with this composition and volatile concentrations can be made by VolatileCalc (Newman and Lowenstern, 2002), and give values ~250 MPa for the saturation of a multi-component (H_2O - CO_2) gas phase in equilibrium with the volatiles dissolved in the magma at 1100°C. This means that such magmas were able to exsolve a H_2O -bearing gas phase just below 6 km of depth. These conditions could be viewed as the triggering mechanism of processes already recognized in literature, defined as volatile-induced differentiation or volatile transfer (Rittmann, 1962; Burnham, 1979; Caroff *et al.*, 1997; De Hoogh and Van Bergen, 2000; Greenough *et al.*, 1999). In magmatic systems, the combined action of water and halogens in complexing and carrying some elements strongly depends on P and T gradients. If volatile exsolution occurs, gases will encounter decreasing P and T conditions during their upward migration: as reactions of metal-

halogens complexing are endothermic, this means that elements carried by a gas phase can be re-dissolved in a magma at shallower levels, leading to a volatile enrichment in the upper portions of magma storage zones. Considering the same degree of differentiation (almost constant SiO_2 and MgO) and the anomalous enrichment in some elements, namely Ti, Fe, P, K and chlorine, the changes in composition recognized in the residual glasses found in tephra erupted at the Laghetto vent could be therefore due to volatile-induced differentiation processes, driven by chemical and physical gradients between the magma bodies within the Etnan plumbing system. Experimental results are fundamental to assess how this selective enrichment may occur. According to Beermann *et al.* (2006) and Stelling *et al.* (2008), the fluid/melt partitioning and solubility of Cl in Etnan trachybasalts of the 2001 eruption, at $T = 1150^\circ C$, $P = 200$ MPa and $fO_2 = QFM + 1$, strongly depends on the formation of complexes of K and other elements (like Ti and Fe) extracted from the melt into the gas phase.

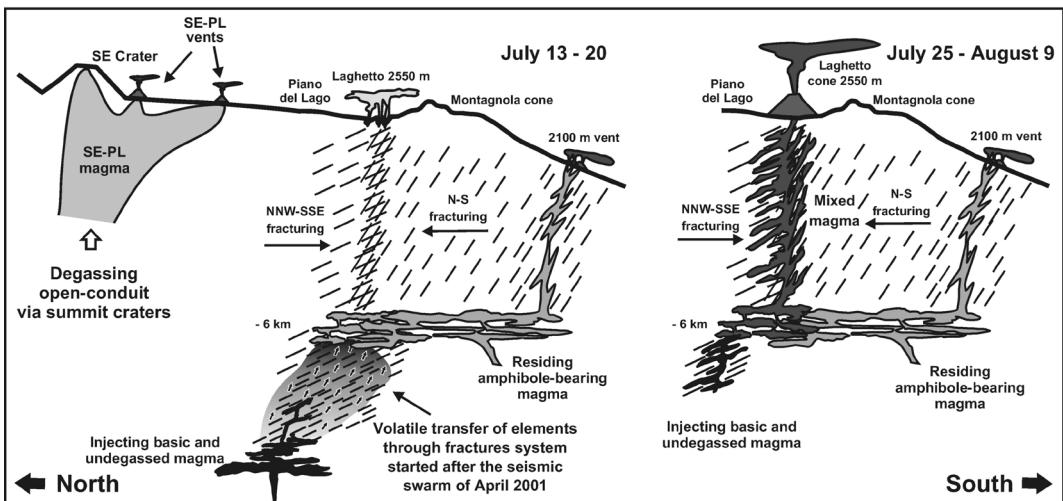


Fig. 5 – Sketch section of the feeding system prior and during the 2001 eruption at Mt. Etna. Volatiles (represented by the shaded cloud and black arrows) exsolved from a more primitive, undegassed magma and migrated upward through fractures probably opened after the April 20 seismic swarm, carrying Cl-complexes of Ti, Fe, P and K. This first phase of magma-volatile interaction enriched in these elements the portions of the residing amphibole-bearing magma last erupted at the Laghetto vent. The 2001 eruption started on July 13 at the South East crater and on July 18 at the 2100 m vent. During the first days, until July 20, the activity took place exclusively at the 2100 m and SE-PL vents. On July 20, the NNW-SSE and N-S fracture systems intersected in the Laghetto area at ~2550 m and phreatomagmatic activity began here; the purely magmatic eruption from the Laghetto vent started on July 25.

Table 5 — Major element abundances (wt.%) for residual glasses in tephra grains from the 2100 m and Laghetto vents of the 2001 eruption (data from Ferlito et al., 2008a)

	Sample	SiO ₂	TiO ₂	Al ₂ O ₃	FeO	MgO	MnO	CaO	Na ₂ O	K ₂ O	P ₂ O ₅	Total	Cl
2100 m lower layers	CAL1-1	50.99	1.96	16.46	10.72	3.31	0.21	7.53	4.19	3.34	1.05	99.77	0.21
	CAL1-2	50.95	1.91	16.64	10.71	3.27	0.14	7.46	4.32	3.52	0.82	99.74	0.22
	CAL1-3	50.87	2.13	16.70	10.46	3.24	0.20	7.44	4.22	3.56	0.95	99.79	0.17
	CAL1-4	51.00	2.02	16.64	10.58	3.26	0.16	7.50	4.25	3.40	0.97	99.78	0.19
	CAL1-5	50.90	1.99	16.38	10.83	3.20	0.26	7.45	4.36	3.50	0.91	99.79	0.18
	CAL1-6	51.02	2.01	16.64	10.87	3.22	0.15	7.45	3.99	3.49	0.90	99.74	0.21
	CAL1-7	51.12	1.97	16.68	10.51	3.22	0.18	7.35	4.30	3.52	0.93	99.77	0.20
	CAL1-8	51.17	2.00	16.63	10.46	3.07	0.20	7.44	4.32	3.66	0.91	99.85	0.14
	CAL1-9	50.80	1.98	16.76	10.50	3.29	0.16	7.50	4.36	3.49	0.91	99.76	0.21
	CAL1-10	51.20	2.04	16.81	10.81	3.16	/	7.40	3.89	3.65	0.87	99.83	0.14
Laghetto middle layers	LAG3-1	51.80	2.17	17.03	10.90	3.36	0.15	6.34	3.23	3.92	0.93	99.84	0.17
	LAG3-2	51.48	2.16	17.04	11.05	3.22	0.21	6.01	3.56	4.01	0.98	99.73	0.26
	LAG3-3	52.18	1.91	16.92	11.22	3.23	0.16	6.46	2.90	3.95	0.85	99.80	0.19
	LAG3-4	51.37	1.85	16.58	11.34	3.39	/	5.82	4.11	4.65	0.91	100.01	0.21
	LAG3-5	50.51	1.94	18.16	10.71	2.99	/	6.19	4.19	4.19	1.13	100.00	0.18
	LAG3-6	51.96	2.08	16.84	10.73	3.33	/	6.93	2.67	4.13	1.11	99.78	0.20
	LAG3-7	51.68	1.99	16.86	11.38	3.26	0.24	6.60	2.74	4.10	0.98	99.82	0.20
	LAG3-8	51.66	2.18	16.96	11.22	3.36	0.28	6.05	3.26	3.93	0.84	99.74	0.24
	LAG3-9	51.47	1.99	16.82	10.72	3.17	0.16	7.29	3.41	3.85	0.88	99.76	0.24
	LAG3-10	51.72	2.04	16.91	11.00	3.20	0.19	6.25	3.35	4.06	1.03	99.75	0.24
	LAG3-11	51.60	2.04	16.77	10.71	3.19	0.26	7.80	2.83	3.62	0.98	99.80	0.20
	LAG3-12	52.22	2.09	17.01	10.92	3.09	0.22	7.11	2.52	3.64	0.98	99.80	0.20
	LAG3-13	51.69	2.18	17.08	11.31	3.27	0.30	7.16	2.35	3.62	0.91	99.86	0.14
	LAG3-14	52.04	2.03	17.15	10.86	3.28	0.19	6.16	3.12	4.07	0.90	99.81	0.18
	LAG3-15	51.93	2.16	16.99	11.07	3.27	/	6.59	3.05	3.90	0.86	99.81	0.19
Laghetto top layers	LAG7-1	51.46	2.14	16.52	10.98	3.17	0.20	6.47	3.03	4.85	0.91	99.74	0.28
	LAG7-2	51.42	2.11	16.63	10.85	3.09	/	5.53	3.84	5.38	0.93	99.79	0.27
	LAG7-3	51.74	2.11	16.65	11.53	3.57	0.18	4.54	3.15	5.23	1.02	99.73	0.30
	LAG7-4	51.14	2.07	16.99	11.30	2.67	/	5.06	4.27	5.39	0.89	99.78	0.26
	LAG7-5	50.15	2.14	16.45	10.90	2.76	0.16	6.91	4.31	5.06	0.91	99.75	0.29
	LAG7-6	51.65	2.26	16.77	11.27	3.36	0.26	5.46	2.85	4.83	0.97	99.69	0.33
	LAG7-7	50.81	2.19	16.52	11.43	2.99	0.14	6.30	3.44	4.92	1.04	99.78	0.27
	LAG7-8	50.93	2.07	16.54	11.17	2.48	0.24	5.95	4.39	4.97	0.97	99.73	0.30
	LAG7-9	51.95	2.18	16.67	10.79	3.12	0.21	6.04	2.97	4.79	1.03	99.74	0.29
	LAG7-10	51.19	2.12	16.58	10.91	3.40	0.28	4.48	4.23	5.56	1.01	99.77	0.29

As a conclusion, after the first phase of magma-fluids interaction, the more primitive, volatile-rich magma rose up to the higher portions of the volcano, and intersected the northern end of a magma batch where the amphibole-bearing trachybasalt was residing. The consequent mixing between the two magmas produced a hybrid member, erupted just at the Laghetto vent (Fig. 5).

Volatile transfer and mixing prior to the 2001 eruption can be viewed as concurring to increase the total volatile content in the magma and to enhance then the gas exsolution. This led to a larger explosivity of the short-lasting eruptive episode at the Laghetto vent, which was one of the most violent in the last centuries. Aim of this comprehensive review, at the scale of a single eruption, is then to stimulate future investigations on uncommon differentiation processes also at other active basaltic volcanoes, since they can be viewed as paramount factors in determining sudden changes of their eruptive behaviour, and therefore of potential hazard.

ACKNOWLEDGEMENTS

Authors are grateful to L. Morbidelli, M. Coltorti and R. Santacroce, who provided perceptive and insightful reviews that improved the early-submitted version of the manuscript. This work has been financially supported by research grants from: MIUR-PRIN 2005: Dynamics of magma ascent and eruptions; INGV-DPC Project V3_6/10 Etna: Plumbing system and structure of the volcano from the lithosphere to the surface; Catania University Research Project 2005: Le manifestazioni eruttive etnee recenti nel quadro del vulcanismo dell'area.

REFERENCES

- ALLARD P., BEHNCKE B., D'AMICO S., NERI M. and GAMBINO S. (2006) - *Mount Etna 1993-2005: anatomy of an evolving eruptive cycle*. Earth Sci. Rev., **78**, 85-114.
- ALLEGRE C.J., PROVOST A. and JAUPART C. (1981) - *Oscillatory zoning: a pathological case of crystal growth*. Nature, **294**, 223-229.
- ARMIENTI P., INNOCENTI F., PETRINI R., POMPILIO M. and VILLARI L. (1989) - *Petrology and Sr-Nd isotope geochemistry of recent lavas from Mt. Etna: bearing on the volcano feeding system*. J. Volcanol. Geotherm. Res., **39**, 315-327.
- ASIMOW P.D. and GHIORSO M.S. (1998) - *Algorithmic modifications extending MELTS to calculate subsolidus phase relations*. Am. Mineral., **83**, 1127-1131.
- BARBIERI M., CRISTOFOLINI R., DELITALA M.C., FORNASERI M., ROMANO R., TADDEUCCI A. and TOLEMO L. (1993) - *Geochemical and Sr-isotope data on historic lavas of Mount Etna*. J. Volcanol. Geotherm. Res., **56** (1-2), 57-69.
- BEERMANN O., STELLING J., NOWAK M. and BOTCHARNIKOV R.E. (2006) - *Partitioning of chlorine between H₂O-bearing fluid and basaltic melt on Mount Etna*. XXVII (14) Arbeitstagung, Modellierungen von Strukturen und Strukturbildungsprozessen in nichtkristallinen Materialien, 28-30 August, Wolfersdorf.
- BEHNCKE B. and NERI M. (2003) - *The July-August 2001 eruption of Mt. Etna (Sicily)*. Bull. Volcanol., **65**, 461-476.
- BRANCA S. and DEL CARLO P. (2004) - *Eruption of Mt. Etna during the past 3200 years: a revised compilation integrating the historical and stratigraphic records*. In: Bonaccorso A., Calvari S., Coltellini M., Del Negro C. and Falsaperla S. (Eds.), Etna volcano laboratory. AGU Geophysical Monograph Series, vol. 143, Washington, D.C., pp. 1-27.
- BURNHAM C.W. (1979) - *Magmas and hydrothermal fluids*. In: Barnes HL (ed) Geochemistry of hydrothermal ore deposits. Wiley, New York, pp. 71-136.
- CAROFF M., AMBRICS C., MAURY R.C. and COTTON J. (1997) - *From alkali basalt to phonolite in hand-size samples: vapor-differentiated effects in the Bouzentes lava flow (Cantal, France)*. J. Volcanol. Geotherm. Res., **79**, 47-61.
- CASHMAN K.V. (1990) - *Textural constraints on the kinetics of crystallization of igneous rocks*. Rev. Mineral., **24**, 259-314.
- CLOCCHIATTI R., CONDOMINES M., GUÉNOT N. and TANGUY J.C. (2004) - *Magma changes at Mount Etna: the 2001 and 2002-2003 eruptions*. Earth Planet. Sci. Lett., **226**, 397-414.
- CONDOMINES M., TANGUY J.C. and MICHAUD V. (1995) - *Magma dynamics at Mt Etna: constraints from U-Th-Ra-Pb radioactive disequilibria and Sr isotopes in historical lavas*. Earth Planet. Sci. Lett., **132**, 25-41.
- CORSARO R.A. and POMPILIO M. (2004) - *Magma dynamics in the shallow plumbing system of Mt. Etna as recorded by compositional variations in volcanics of recent summit activity (1995 – 1999)*. J. Volcanol. Geotherm. Res., **137**, 55-71.

- CORSARO R.A., CRISTOFOLINI R., FERLITO C., MAZZOLENI P., MIRAGLIA L. and VICCARO M. (2005) - *Quartzarenite xenoliths from recent activity at Mount Etna: evidence of magma-rock interactions in a shallow magma reservoir.* 5° Forum Italiano di Scienze della Terra, Spoleto (Pg) 19-20 Settembre, Epitome, **1**, 284.
- CORSARO R.A., MIRAGLIA L. and POMPILIO M. (2007) - *Petrologic evidence of a complex plumbing system feeding the July-August 2001 eruption at Mt. Etna, Sicily, Italy.* Bull. Volcanol., **69**, 401-421.
- CRISTOFOLINI R. and TRANCHINA A. (1980) - *Aspetti petrologici delle vulcaniti etnee: caratteri dei fenocristalli isolati ed in aggregati.* Rend. Soc. It. Mineral. Petrol., **36**, 751-773.
- CRISTOFOLINI R., SCRIBANO V. and TRANCHINA A. (1981) - *Interpretazione petrogenetica di variazioni composizionali in fenocristalli femici di lava etnea.* Rend. Soc. It. Mineral. Petrol., **31**, 309-336.
- DE HOOGH J.C.M. and VAN BERGEN M.J. (2000) - *Volatile-induced transport of HFSE, REE, Th and U in arc magmas: evidence from zirconolite-bearing vesicles in potassic lavas of Lewotolo volcano (Indonesia).* Contr. Mineral. Petrol., **139**, 485-502.
- DUNCAN A.M. and PRESTON R.M.F. (1980) - *Chemical variation of clinopyroxene phenocrysts from the trachybasaltic lavas of Mount Etna, Sicily.* Mineral. Mag., **43**, 765-770.
- FERLITO C., VICCARO M. and CRISTOFOLINI R. (2008a) - *Volatile-induced differentiation in the plumbing system of Mt. Etna volcano (Italy): evidence from glass in tephra of the 2001 eruption.* Bull. Volcanol., **70**, 455-473.
- FERLITO C., VICCARO M., NICOTRA E. and CRISTOFOLINI R. (2008b) *Relationship between magma supply and eruptive behavior at Mt. Etna volcano during the 2006-2007 period.* EGU General Assembly, Vienna (Austria), 13-18 Aprile, Geophys. Res. Abs., **10**, 03386, SRef-ID: 1607-7962/gra/EGU-A-03386.
- GHIORSO M.S. and SACK R.O. (1995) - *Chemical mass transfer in magmatic processes 4. A revised and internally consistent thermodynamic model for the interpolation and extrapolation of liquid-solid equilibria in magmatic systems at elevated temperatures and pressures.* Contr. Mineral. Petrol., **119**, 197-212.
- GREENOUGH J.D., LEE C.Y. and FRYER B.J. (1999) - *Evidence for volatile-influenced differentiation in a layered alkali basalt flow, Penghu Island, Taiwan.* Bull. Volcanol., **60**, 412-424.
- HOLTON T., JAMTVEIT B. and MEAKIN P. (2000) - *Noise and oscillatory zoning of minerals.* Geochim. Cosmochim. Acta, **64**, 1893-1904.
- LE MAITRE R.W. (2002) - *A classification of igneous rocks and glossary of terms.* Cambridge University Press, pp. 1-236.
- L'HEUREUX I. (1993) - *Oscillatory zoning in crystal growth: a constitutional undercooling mechanism.* Phys. Rev. (E), **48**, 4460-4469.
- MÉTRICH N. and RUTHERFORD M.J. (1998) - *Low pressure crystallization paths of H_2O -saturated basaltic-hawaiitic melts from Mt. Etna: implications from open-system degassing of basaltic volcanoes.* Geochim. Cosmochim. Acta, **62**, 1195-1205.
- MÉTRICH N., ALLARD P., SPILLIAERT N., ANDRONICO D. and BURTON M. (2004) - *2001 flank eruption of the alkali- and volatile-rich primitive basalt responsible for Mount Etna's evolution in the last three decades.* Earth Planet. Sci. Lett., **228**, 1-17.
- MONACO C., CATALANO S., COCINA O., DE GUIDI G., FERLITO C., GRESTA S., MUSUMECI C. and TORTORICI L. (2005) - *Tectonic control on the eruptive dynamics at Mt. Etna Volcano (Sicily) during the 2001 and 2002–2003 eruptions.* J. Volcanol. Geotherm. Res., **144**, 211-233.
- MORIMOTO N. (1988) - *Nomenclature of pyroxenes.* Mineral. Petrol., **39**, 55-76.
- NEWMAN S. and LOWENSTERN J.B. (2002) - *VOLATILECALC: a silicate melt- H_2O - CO_2 solution model written in Visual Basic Excel.* Comput. Geosci., **2**, 597-604.
- ORTOLEVA P.J. (1990) - *Role of attachment kinetic feedback in the oscillatory zoning of crystals grown from melts.* Earth Sci. Rev., **29**, 3-8.
- PATANÈ D., CHIARABBA C., COCINA O., DE GORI P., MORETTI M. and BOSCHI E. (2002) - *Tomographic images and 3D earthquake locations of the seismic swarm preceding the 2001 Mt. Etna eruption: evidence for a dyke intrusion.* Geophys. Res. Lett., **29** (135), 1-4.
- RITTMANN A. (1962) - *Volcanoes and their activity.* Wiley and Sons, New York, 305 pp.
- ROMANO R. (1982) - *Succession of the volcanic activity in the Etnean area.* Mem. Soc. Geol. It., **23**, 27-48.
- SISSON T.W. and GROOVE T.L. (1993) - *Experimental investigations of the role of H_2O in calk-alkaline differentiation and subduction zone magmatism.* Contrib. Mineral. Petrol., **113**, 143-166.
- STELLING J., BOTCHARNIKOV R.E., BEERMANN O. and NOWAK M. (2008) - *Solubility of H_2O - and chlorine-bearing fluids in basaltic melt of Mount Etna at $T=1050-1250^\circ C$ and $P=200$ MPa.* Chem. Geol.,

- in press, doi:10.1016/j.chemgeo.2008.04.009.
- TANGUY J.C., CONDOMINES M. and KIEFFER G. (1997) - *Evolution of Mount Etna magma: Constraints on the present feeding system and eruptive mechanism.* J. Volcanol. Geotherm. Res., **75**, 221-250.
- TONARINI S., ARMIENTI P., D'ORAZIO M. and INNOCENTI F. (2001) - *Subduction-like fluids in the genesis of Mt. Etna magmas: evidence from boron isotopes and fluid mobile elements.* Earth Planet. Sci. Lett., **192**, 471-483.
- VICCARO M. and CRISTOFOLINI R. (2008) - *Nature of mantle heterogeneity and its role in the short-term geochemical and volcanological evolution of Mt. Etna (Italy).* Lithos, **105**, 272-288.
- VICCARO M., FERLITO C., CORTESOGNO L., CRISTOFOLINI R. and GAGGERO L. (2006) - *Magma mixing during the 2001 event at Mount Etna (Italy): effects on the eruptive dynamics.* J. Volcanol. Geotherm. Res., **149**, 139-159.
- VICCARO M., FERLITO C. and CRISTOFOLINI R. (2007) - *Amphibole crystallization in the Etmean feeding system: mineral chemistry and trace element partitioning between Mg-hastingsite and alkali basaltic melt.* Eur. J. Mineral., **19**, 499-511.